Laboratory Investigation (2020) 100:959–973
https://doi.org/10.1038/s41374-020-0419-2

ARTICLE

Elk-1 transcriptionally regulates ZC3H4 expression to promote silica-induced epithelial–mesenchymal transition

Rong Jiang[1] · Qianqian Gao[2] · Mingxia Chen[1] · Tingting Yu[3]

Received: 8 October 2019 / Revised: 9 March 2020 / Accepted: 11 March 2020 / Published online: 26 March 2020

Abstract

The epithelial–mesenchymal transition (EMT) process is a key priming activity of fibroblasts in pulmonary fibrosis during silicosis. Ets-like protein-1 (Elk-1) is a critical modulator that promotes functional changes in cells, and the effects are mediated by oxidative stress (OS). However, whether ELK-1 is involved in EMT of silicosis remains unclear. In addition, researchers have found that Elk-1 is involved in the expression of the gene *zc3h12a*, which encodes the protein MCPIP1, and MCPIP1 is a member of the zinc finger Cys-Cys-Cys-His (CCCH)-type protein family. A previous study from our lab showed that ZC3H4, which is also a member of the CCCH-type protein family, critically affected the regulation of EMT during silicosis. However, it has not yet been elucidated if ELK-1 acts at the promoter for *zc3h4* to increase its expression in a mechanism that is similar to that of the *zc3h12a* gene and whether such regulation ultimately controls EMT. Therefore, we explored the correlation between ELK-1 and ZC3H4 expression and tested the underlying mechanisms affecting ELK-1 activation induced by silica. Our study identifies that SiO_2-mediated EMT via ELK-1, with the upstream activity of OS and the downstream signaling of ZC3H4 expression resulting in enhanced EMT. These findings suggest that the nuclear transcription factor ELK-1 may be useful as a novel target for the treatment of pulmonary fibrosis.

Introduction

Silicosis is a systemic disease caused by long-term inhalation of a high concentration of free silicon dioxide (SiO_2) particles, and it is characterized by pulmonary fibrosis and silicon nodule formation [1]. It is one of the occupational diseases with the highest incidence rates, displaying the features of hidden incidence, a long incubation period, and complex presentation [2, 3]. Pulmonary injuries develop progressively, even after escaping the occupational exposure [2, 4].

The cellular mechanisms of silicosis include abnormal activation of macrophages, oversecretion of inflammatory cytokines or fibrogenic factors, including transforming growth factor-β (TGF-β) [5–8], severe destruction of pulmonary alveolar epithelial cells and vascular endothelial cells, occurrence of epithelial–mesenchymal transition (EMT), and endothelial–mesenchymal transition; these activities result in excessive myofibroblast proliferation and extracellular matrix over-deposition [9–11]. Notably, EMT, which is characterized by the loss of epithelial cell junction proteins, such as E-cadherin (E-cad), and the upregulation of mesenchymal markers, such as collagen I (COL1), vimentin, and N-cadherin, was recently considered to be a vital source of tissue myofibroblasts [12]. It has been well-established that multiple biological processes are critical for EMT, and oxidative stress (OS) is a crucial molecular mechanism leading to EMT [13, 14]. The inhalation of silica particles has been shown to stimulate the production of reactive oxygen species (ROS) as a part of the persistent fibrotic responses associated with EMT [15]. EMT has been implicated in the pathogenesis of lung fibrosis in response to epithelial injury. Previous studies from our lab have also

Supplementary information The online version of this article (https://doi.org/10.1038/s41374-020-0419-2) contains supplementary material, which is available to authorized users.

✉ Rong Jiang
jiangrong@njmu.edu.cn

[1] Department of Clinical Nursing, School of Nursing, Nanjing Medical University, Nanjing, Jiangsu, China

[2] Department of Occupation Disease Prevention and Cure, Center for Disease Control and Prevention, Nanjing 210009 Jiangsu, China

[3] Intensive Care Unit, The First People's Hospital of Kunshan, Kunshan 215300 Jiangsu, China

reported that EMT plays a crucial role in the pathogenesis of pulmonary fibrosis induced by silica [9].

Substantial evidence has indicated that multiple transcription factors, such as TWIST-1, snail, and ZEBs, are involved in the complex pathogenesis of EMT states [16]. Among these, snail acted as a repressor of E-cad expression and an inducer of EMT in various types of epithelial cells [17, 18]. A recent study has demonstrated that Ets-like protein-1 (Elk-1) is involved in the EMT process by modulating *snail* gene expression through the extracellular signal-regulated kinase (ERK) pathway [19, 20]. ELK-1 is a well-studied member of the ternary complex factor (TCF) family, which binds to target gene sequence promoters together with serum response factor (SRF) to form ternary complexes called serum response elements (SREs) [21]. The transcriptionally active form of ELK-1 is characterized by the de-SUMOylation and phosphorylation of serine or threonine residues at COOH-terminal sites. The phosphorylation of Elk-1 (p-ELK-1), which is induced by ERK1/2, leads to Elk-1 translocation from the cytoplasm to the nucleus and also results in the regulation of SRE-dependent transcription by chromatin remodeling [22]. Transcriptional activity is stimulated by different mitogen-activated protein kinase (MAPK) signaling pathways. Mounting evidence has demonstrated that OS induces activation of MAPK signaling pathways, such as ERK, p38 MAPK, and c-Jun N-terminal kinase pathways [23]. These pathways can mediate the activation of a wide variety of transcription factors and cellular processes, including cell differentiation, proliferation, survival, adhesion, and migration [24]. However, whether OS modulates the activation of ELK-1, mediating EMT and EMT-related functional changes remains poorly understood.

The immediate-early genes (IE genes), such as FOS and EGR1, that are engaged in expressing signaling pathway factors are activated by the Elk-1 transcription factor with rapid activation kinetics [25]. Moreover, Elk-1 is also implicated in the expression of IE genes encoding proteins critical for transcript turnover, namely, *zc3h12a*, which encodes the Zinc finger Cys-Cys-Cys-His (CCCH) type protein MCPIP1. The structures of a CArG box (binding site for the transcription factor SRF) and an Ets-binding site (binding site for Elk-1) in the *zc3h12a* gene promoter cause phosphorylated ELK-1 to bind strongly to *zc3h12a* [25, 26]. Based on our earlier studies, we clearly demonstrated the role of another newly identified member from the zinc finger CCCH-type protein family, zinc finger CCCH-type containing 4 protein (ZC3H4), in cellular phenotypic changes during silicosis [9, 27]. Because ZC3H4 is a member of the same family as ZC3H12A, we speculated that the *zc3h4* gene promoter contained a hypothetical binding site for ELK-1, such as a CArG box, which enables a novel hypothesis that ELK-1 may bind to the *zc3h4* gene promoter and activate transcription, ultimately controlling ZC3H4 protein expression as well as the EMT process during silicosis.

To elucidate the role of ELK-1 in silica-induced EMT, we knocked down ELK-1 expression and detected the functional behaviors related to EMT. Herein, we demonstrated that the connections between OS and the activation of ELK-1 and ZC3H4 are involved in the regulation of EMT and TGF-β production. These findings identified a new function for ELK-1 in pulmonary epithelial cells and suggested that ELK-1 may be involved in multiple steps of pulmonary fibrosis.

Materials and methods

Reagents

Eighty percent of the SiO_2 particles were between 2 and 5 μm in diameter, and they were purchased from Sigma® (S5631). The SiO_2 particles were sterilized overnight as previously described (200 °C for 16 h) [28], and they were then diluted in sterilized phosphate buffer solution (PBS) or normal saline (NS) at a concentration of 5 or 50 mg/ml, respectively. The SiO_2 dosage used in cellular or animal experiments was the same as our experimental results (Fig. S1) and what was used in our previous studies [27]. N-acetylcysteine (NAC) was bought from the Beyotime (S0077) company. Antibodies against ZC3H4 (20041-1-AP), α-SMA (14395-1-AP), and TGF-β(18978-1-AP) were bought from Protein tech company. Antibodies against p-ELK-1 (SC-8406, mouse) and E-cad (sc-9989, mouse) were bought from Santa Cruz Biotechnology, Inc.

Cell culture

Mouse lung epithelial-12 (MLE-12) cells and human pulmonary epithelial cell-BEAS-2B cells were obtained from ATCC®, and they were cultured in dulbecco's modified eagle medium (DMEM) containing 10% fetal bovine serum (FBS) at 5% CO_2 and 37 °C. The cells used in the experiments were between passages 5 and 15.

Animal model establishment

C57BL/6J mice were purchased from the Model Animal Research Center of Nanjing Medical University. C57BL/6J mice were 5–8 weeks old and were administered abdominal pentobarbital sodium for anesthesia. After basic anesthesia, the mice were administered a SiO_2 suspension (5 mg particles in 100 μL of NS) via the trachea a single time, and the control group was treated with 100 μL of sterilized NS [28]. Pulmonary tissues were obtained after SiO_2 suspension treatment for 28 days.

Western blot analysis

Western blot analysis was measured as previously reported [29]. Briefly, the cells were collected in RIPA lysis buffer (P0013B, Beyotime) after being washed several times with cold PBS buffer. Nuclear and cytoplasmic proteins were extracted using an extraction kit (P0027, Beyotime). The concentration of each sample was detected using a BCA kit (P0011, Beyotime). Equal concentrations of each sample were separated by 8–12% SDS-PAGE and were transferred to PVDF membranes. PVDF membranes were incubated in 5% nonfat dry milk for 1 h under ambient conditions. After that, the membranes were incubated with the primary antibodies against glyceraldehyde-3-phosphate dehydrogenase (GAPDH), α-SMA, E-cad, ZC3H4, p-ELK-1, and Histone H3 (1:800) at 4 °C for a whole night. The next day, the membrane was washed and then incubated for 1 h with secondary antibodies conjugated with horseradish peroxidase (Thermo Fisher Scientific). Protein bands were visualized using a chemiluminescent reagent (SuperSignal West Femto Maximum Sensitivity Substrate; Thermo Fisher Scientific) and a Kodak IS4000 MM Pro Imaging System (Carestream Health, Rochester, NY). Each Western blot was representative of at least five independent experiments. The protein bands were evaluated using ImageJ 1.48v software.

Immunofluorescence staining

Immunofluorescence staining was conducted as previously described [30].

Cell transfection via CRISPR-associated protein 9 (Cas9) technology

The CRISPR/Cas9 knockout plasmids (sc-437281, sc-400385-NIC, sc-420156-NIC, sc-436020-NIC, and sc-411693-NIC) and the CRISPR activation plasmids (sc-437275, sc-400385-ACT, sc-420156-ACT, sc-436020-ACT, and sc-411693-ACT) were obtained from Santa Cruz Biotechnology. The transfection volume listed here was for a single well of a 24-well cell-culture plate. Transient transfection was conducted as previously described [27].

Oxidative damage assessment

Intracellular ROS levels were measured by a Reactive Oxygen Species Assay kit (Beyotime, China) with the fluorescent probe dichlorofluorescein diacetate (DCFH-DA); the enzyme activity of total superoxide dismutase (SOD) was measured by a Total Superoxide Dismutase Assay kit with WST-8 (Beyotime); the enzyme activity of glutathione (GSH) was measured by a GSH and a GSSG Assay kit (Beyotime). Concentrations of SOD and GSH were expressed as unit per milligram of total protein [31]. All indexes were detected according to the manufacturers' instructions.

Cell Counting Kit-8 assay

Cell viability was performed via Cell Counting Kit-8 (K1018, Apexbio), which was reported in a previous research [32].

Bromodeoxyuridine (BrdU) labeling

Cell proliferation ability was evaluated via the BrdU assay, which was reported in a previous research [29].

Nested matrix model and three-dimensional cell migration assay

Three-dimensional (3D) cell migration assays were conducted as in previous research with a few improvements [33]. A nested collagen matrix model was established to provide an adhesive state for 3 days of culture in DMEM containing 5% FBS. The matrix was then removed from the culture well and covered with 60 μL of fresh acellular collagen matrix solution (NeoMatrix solution) in the middle area of a new well in a 24-well plate. The newly transferred matrix was used to place 140 μL of fresh acellular collagen matrix solution. The mixture matrix was applied to aggregate for 1 h at a standard culture temperature (37 °C) in an atmosphere of 5% CO_2; next, 1 mL of DMEM containing 10% FBS was added to each well. In these experiments, MLE-12 cells were treated with plasmids or silica dioxide according to the group. The cells that migrated out of or into the mixture matrix were evaluated via fluorescence microscopy at 0, 12, 24, and 48 h and then were compared with the control group. We used fluorescence microscopy (EVOS® FL, Life Technologies) to capture the digital pictures. The migration ability of MLE-12 cells was examined by counting the numbers of migrated cells that migrated from the interface of the nested matrix into the cell-free matrix. The numbers of migrated cells were averaged from five randomly selected microscopic fields for each group.

Quantitative RT-PCR

Quantitative RT-PCR analysis was used to examine mRNA expression. Total RNA was isolated from MLE-12 cells using TRIzol reagent (Thermo Fisher Scientific). The concentration of RNA was evaluated by a NanoDrop-One system (Thermo Fisher Scientific). Following the determination of the concentration of RNA, 400 ng of total RNA was reverse transcribed to generate cDNA. The products of

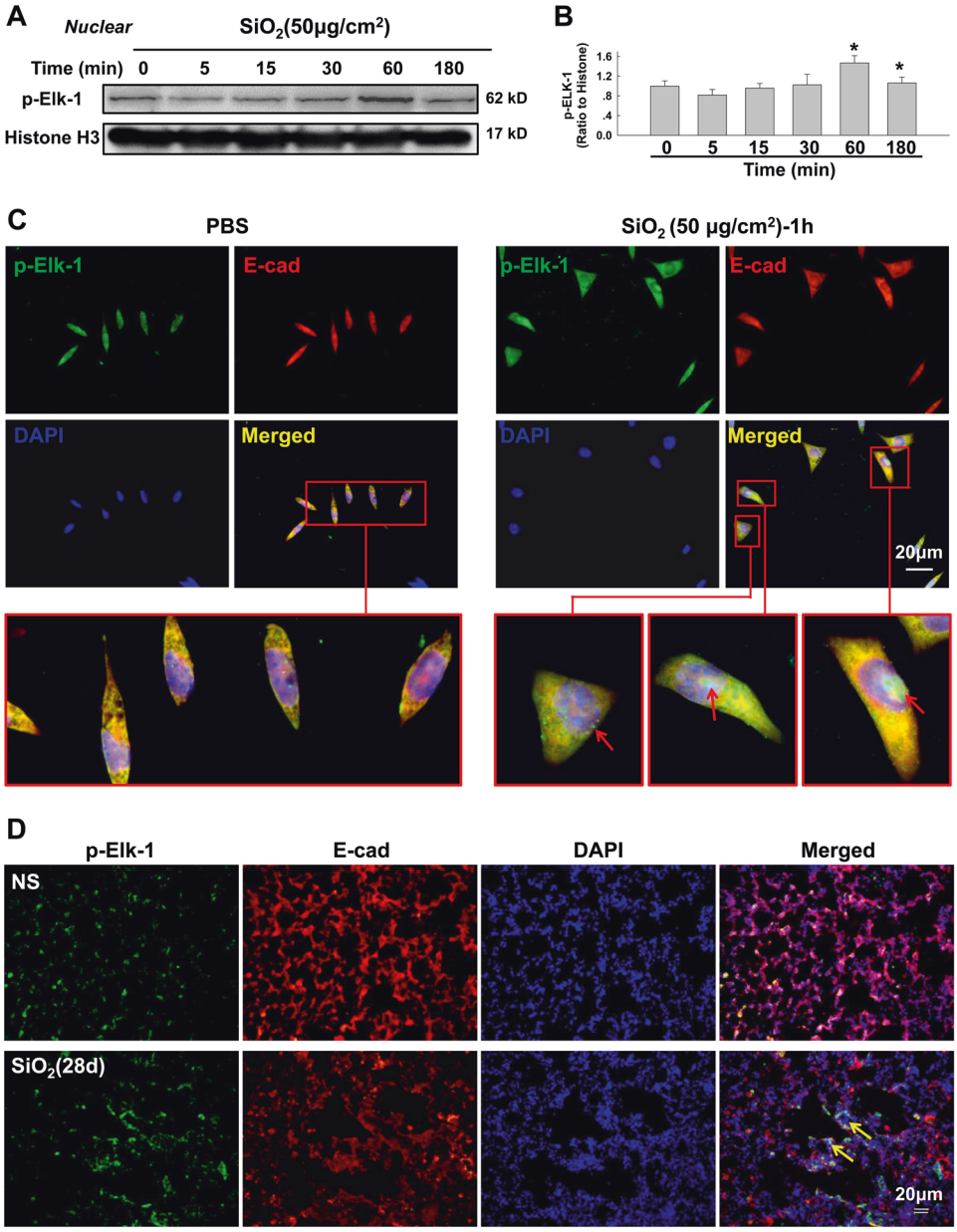

Fig. 1 SiO_2 increases the activation of ELK-1. **a** Representative western blots showing SiO_2 stimulates Elk-1 phosphorylation in the nucleus of MLE-12 cells. **b** Densitometric analyses of Elk-1 phosphorylation ($n = 5$); $^*p < 0.05$ vs. the 0-h group. **c** Representative immunofluorescence staining images illustrating that SiO_2 decreases the expression of E-cad and increases the Elk-1 phosphorylation and nuclear translocation in MLE-12 cells. Nuclei are stained using DAPI. The arrowhead signal points indicate Elk-1 phosphorylation and nuclear translocation induced by SiO_2. Scale bar = 20 μm. **d** Representative immunofluorescence staining images showing E-cad expression and Elk-1 phosphorylation in lung tissues from normal saline (NS)-treated mice and SiO_2-treated mice, E-cad expression is decreased, while Elk-1 phosphorylation and nuclear translocation are increased in silicosis group. Nuclei are stained using DAPI. The arrowhead indicates the colocation signals of E-cad and p-Elk-1 induced by SiO_2. The images are representative of several mice from each group ($n = 6$). Scale bar = 20 μm.

reverse transcription acted as templates for qRT-PCR. The intersection points of the amplification curve and the threshold lines were used to examine the relative quantitative expression of RNA. The relative quantitative levels of RNA were normalized to GAPDH.

Statistics

The data analyses were performed using SigmaPlot 11.0 software. The data are presented as the mean ± standard error of the mean (SEM). Unpaired *t*-test (two groups) or analysis of variance (greater than two groups) were used to calculate the significant differences. $P < 0.05$ was used to analyze the significant differences.

Results

SiO_2 increased the activation of ELK-1

Because reactive pulmonary epithelial cells always exhibit high viability [34, 35], we first explored the effects of various concentrations of SiO_2 on cell viability. The pulmonary epithelial cells, MLE-12 and BEAS-2B, were treated with different concentrations of SiO_2 for 24 h, which was followed by cell viability assessment. As shown in Fig. S1A, B, the CCK8 assay results indicated that SiO_2 increased the viability of epithelial cells in a dose-dependent manner. SiO_2 at a concentration of 50 μg/cm^2 significantly increased the cell viability of MLE-12 and BEAS-2B cells,

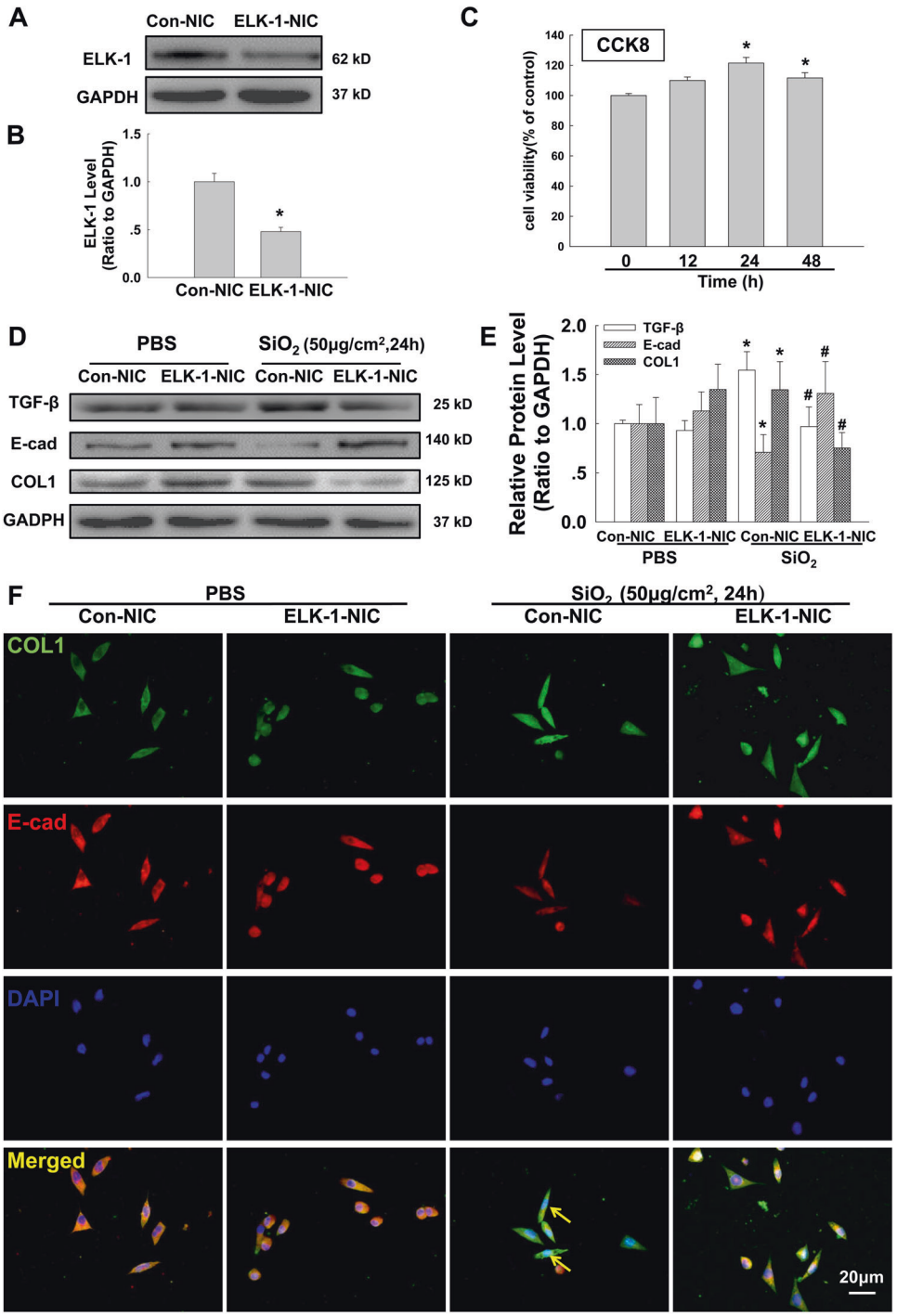

Fig. 2 ELK-1 is involved in SiO_2-induced EMT and TGF-β production. a Representative western blots showing that transfection downregulates ELK-1 expression in MLE-12 cells using the CRISPR/Cas9 system. **b** Densitometric analyses of five separate experiments suggest that transfection with ELK-1 double nickase plasmid (ELK-1 NIC) downregulates ELK-1 expression in MLE-12 cells; $^{*}p < 0.05$ vs. the control group. **c** CCK8 assay showing the effects of SiO_2 on the viability of MLE-12 cells in a time-dependent manner.$^{*}p < 0.05$ vs. the 0-h group. **d** Representative western blots showing that downregulating ELK-1 inhibits SiO_2-induced increase in Col I and TGF-β expression, while reverses the SiO_2-induced decrease in E-cad expression in MLE-12 cells. **e** Densitometric analyses of five independent experiments showing Col I, TGF-β, and E-cad expression ($n = 5$); $^{*}p < 0.05$ vs. the control group; $^{\#}p < 0.05$ vs. the SiO_2 group. **f** Representative immunofluorescence staining images demonstrating that SiO_2 decreases the expression of E-cad and increases the expression of Col I in MLE-12 cells. While CRISPR/Cas9-mediated ELK-1 silencing attenuates the SiO_2-induced increase in Col I expression and ameliorates the SiO_2-induced decrease in E-cad expression. The arrowhead indicates the morphology change induced by SiO_2. Scale bar = 20 μm.

while 200 μg/cm^2 SiO_2 exhibited a toxic effect on cells compared with the other groups. Therefore, we chose 50 μg/cm^2 for the rest of the in vitro assays.

To explore the potential transcription factors involved in cell activation, we first investigated the effect of SiO_2 on Elk-1 expression. Both phosphorylation at COOH-terminal sites and nuclear translocation are critical for the transcriptional potential of ELK-1 [36, 37]. As shown in Figs. 1a, b and S2A, B, treating MLE-12 and BEAS-2B cells with SiO_2 significantly increased the p-Elk-1 in the nucleus of cells, and it peaked after ~30–60 min of exposure to SiO_2 before tapering off, which was verified by western blotting experiments. The immunofluorescence staining showed that MLE-12 and BEAS-2B cells expressed higher levels of endogenous p-Elk-1 (green fluorescent signal points, arrowhead) in the nucleus within 1 h of SiO_2 administration (Figs. 1c and S2C). To determine whether the p-Elk-1 expression is altered in vivo, C57BL/6J mice

were treated with SiO_2 via intratracheal injection to establish mouse models of silicosis as was performed in a previous study [28]. Previous studies have demonstrated that EMT was induced by exposure to SiO_2 for 28 days in vivo. Under conditions of EMT, we examined the p-Elk-1 and observed colocalization between p-Elk-1 and the epithelial cell marker E-cad in lung tissues. In accordance with the in vitro results, immunohistofluorescence staining (Fig. 1d) of lung tissues showed the colocalization of p-Elk-1 and E-cad (arrowhead). Compared with the control group, alveolar damage was more serious, p-Elk-1 was expressed robustly, and there was a lower level of E-cad expression in the pulmonary parenchyma of the experimental group. Taken together, these results revealed that SiO_2 stimulated rapid ELK-1 activation, which was characterized by increased nuclear translocation and phosphorylation.

ELK-1 was involved in SiO_2-induced EMT and TGF-β production

In order to explore the regulation role of ELK-1 on EMT, the CRISPR/Cas9 NIC system was used to knock down ELK-1 expression specifically (Fig. 2a, b). Since a previous study from our lab found that SiO_2 induced the expression of EMT markers in a time-dependent manner in MLE-12 and BEAS-2B cells with a peak response at 24 h [9]. What's more, SiO_2 increased the viability of MLE-12 and BEAS-2B cells, with the peak response observed at 24 h (Figs. 2c, S1C). Thus, the 24 h time point after SiO_2 exposure was selected to maximize the probability of detecting the effects of ELK-1 because this time point corresponded to the relatively marked EMT phenomenon in MLE-12 and BEAS-2B cells after SiO_2 exposure [9]. As shown in Fig. 2d, e, transfection of the Elk-1 NIC plasmid alone had no effect on the expression of E-cad and Col I, while knocking down Elk-1 protein expression reversed the downregulation of E-cad expression and the upregulation of Col I expression induced by SiO_2. This phenomenon was in accordance with fluorescence staining, from which the fibroblast-shaped morphological changes (arrowhead) induced by SiO_2 were also inhibited in epithelial cells by treatment with the Elk-1 NIC plasmid (Fig. 2f).

The production of TGF-β from lung epithelial cells is a hallmark of the EMT response to fibrogenic reactions [38]. TGF-β is one of the main profibrotic inducers that have been shown to promote EMT and excess collagen deposition in pulmonary fibrosis, which achieves via many different signaling pathways [39]. Therefore, we also performed experiments to evaluate SiO_2-stimulated production of TGF-β. As shown in Fig. 2d, e, SiO_2 treatment for 24 h induced TGF-β expression in epithelial cells; however, transfection with the Elk-1 NIC plasmid abolished the SiO_2-induced increase in TGF-β production. These results indicated that Elk-1 was involved in SiO_2-induced EMT and TGF-β production.

ELK-1 mediated the functional changes in cells that accompany EMT

Accumulating evidence suggests that functional changes in cells are often seen as the first steps of EMT and the subsequent pulmonary fibrosis responses; such changes include cell viability, proliferation, mobility, and so on [12, 40, 41]. The activation of EMT-related cellular functions make it possible for pulmonary alveolar cells to obtain mesenchymal cell characteristics [42]. Increasing evidence has shown that Elk-1 targets genes that encode proteins closely related to cellular functions, such as *ptgs2, hif1a, actb,* and *cdh3*, revealing that Elk-1 may be linked with EMT-related cellular functions [25]. Thus, CCK8 experiments, BrdU experiments, and a 3D culture migration system that facilitate the analysis of epithelial cell physiology under conditions that resemble the in vivo environment were performed to assess the functional relevance of the changes in the ELK-1 expression. Our results showed that SiO_2 dramatically promoted cell viability (Fig. 2c), proliferation (Fig. 3b), and mobility (Fig. 3d, e). Under conditions of functional activation of the cells, we further confirmed the role of ELK-1 on functional changes induced by SiO_2. As shown in Fig. 3, the ELK-1 knockdown group suppressed the increase in cell viability (Fig. 3a), proliferation (Fig. 3c), and migration (Fig. 3d, e) induced by SiO_2 treatment, suggesting that ELK-1 mediated functional changes accompanying EMT.

The relevance between ELK-1 and ZC3H4

Having shown that ZC3H4 played a critical role in EMT induced by SiO_2 [9], we were interested in the connection between ELK-1 and ZC3H4 expression in MLE-12 and BEAS-2B cells after SiO_2 treatment. Thus, we first examined the expression of ZC3H4 protein and mRNA using WB and qRT-PCR experiments, respectively, which showed that under the condition of SiO_2 treatment, knock down of ELK-1 not only attenuated ZC3H4 protein level but also decreased ZC3H4 mRNA level (Figs. 4a–c, S3A–C), implying that ELK-1 mediated *zc3h4* gene expression at the transcriptional level. Concurrently, consistent with the WB results, immunofluorescence staining also confirmed that ZC3H4 expression in MLE-12 cells was downregulated by the ELK-1 NIC plasmids (Fig. 4d). While the results in Fig. 4e, f showed that downregulation of ZC3H4 did not affect the ELK-1 expression, which suggests that there is a strong possibility that ELK-1 is an upstream transcription regulator influencing ZC3H4 protein expression after SiO_2 treatment.

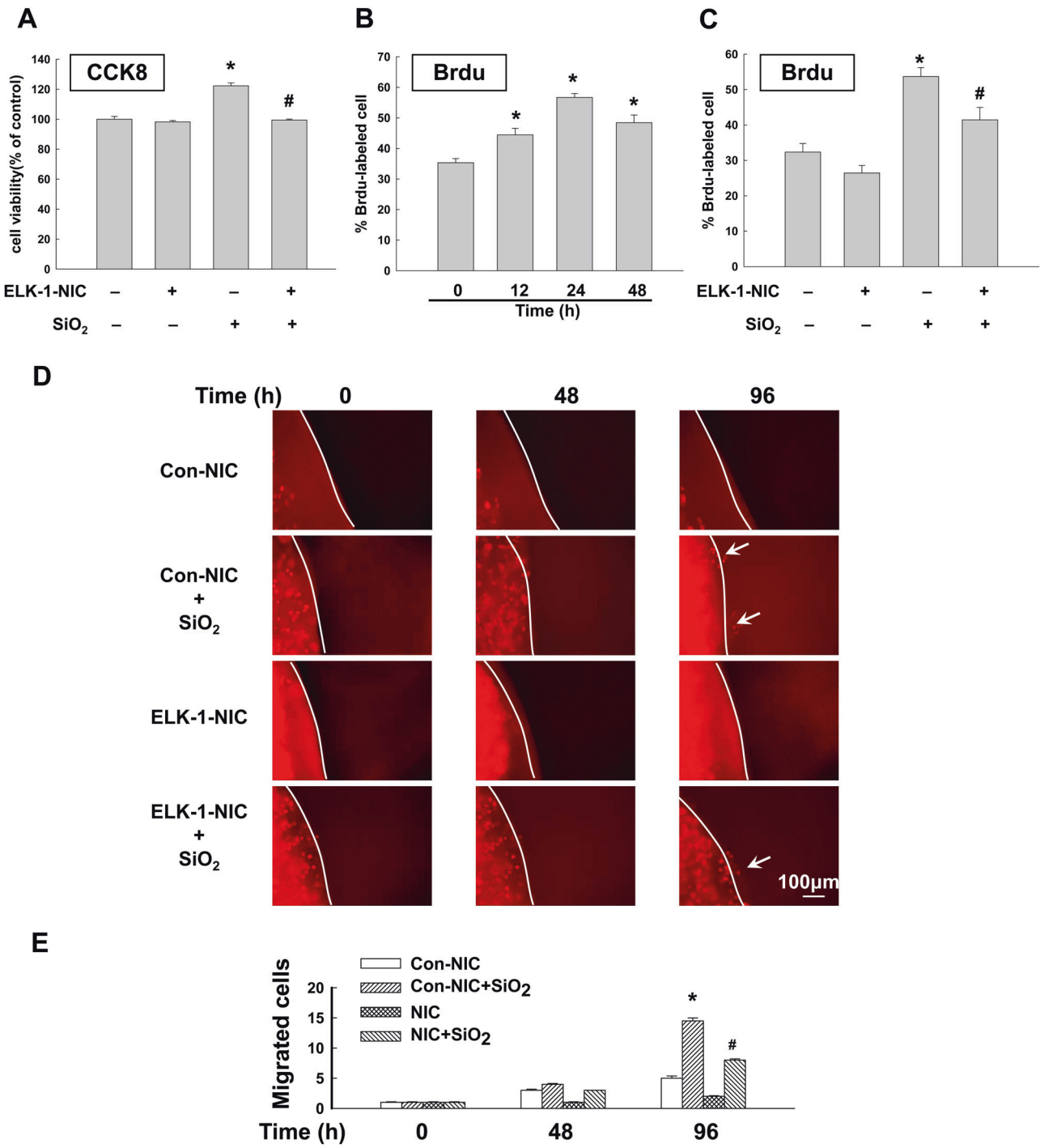

Fig. 3 ELK-1 mediates the related cell functional changes accompanying EMT. a CCK8 assay showing CRISPR/Cas9-mediated ELK-1 silencing inhibits the increased cell viability induced by SiO_2 in MLE-12 cells. $n = 5$; $^{*}p < 0.05$ vs. the control group; $^{\#}p < 0.05$ vs. the SiO_2 group. **b** Brdu positive-cell counting from five fields per well demonstrating the effects of SiO_2 on MLE-12 cells proliferation. $n = 5$; $^{*}p < 0.05$ vs. the 0-h group. **c** Brdu positive-cell counting from five fields per well demonstrating that MLE-12 cells proliferation induced by SiO_2 is attenuated by ELK-1 silencing; $n = 5$; $^{*}p < 0.05$ vs. the control group; $^{\#}p < 0.05$ vs. the SiO_2 group. **d** Representative images demonstrating the SiO_2-induced migration of RFP-labeled MLE-12 cells cultured in a 3D matrix, which is abolished by ELK-1 silencing. Scale bar = 100 μm. **e** Quantification of the number of migrated cells in the 3D migration from six independent experiments. $^{*}p < 0.05$ vs. the control NIC group. $^{\#}p < 0.05$ vs. the control NIC + SiO_2 group.

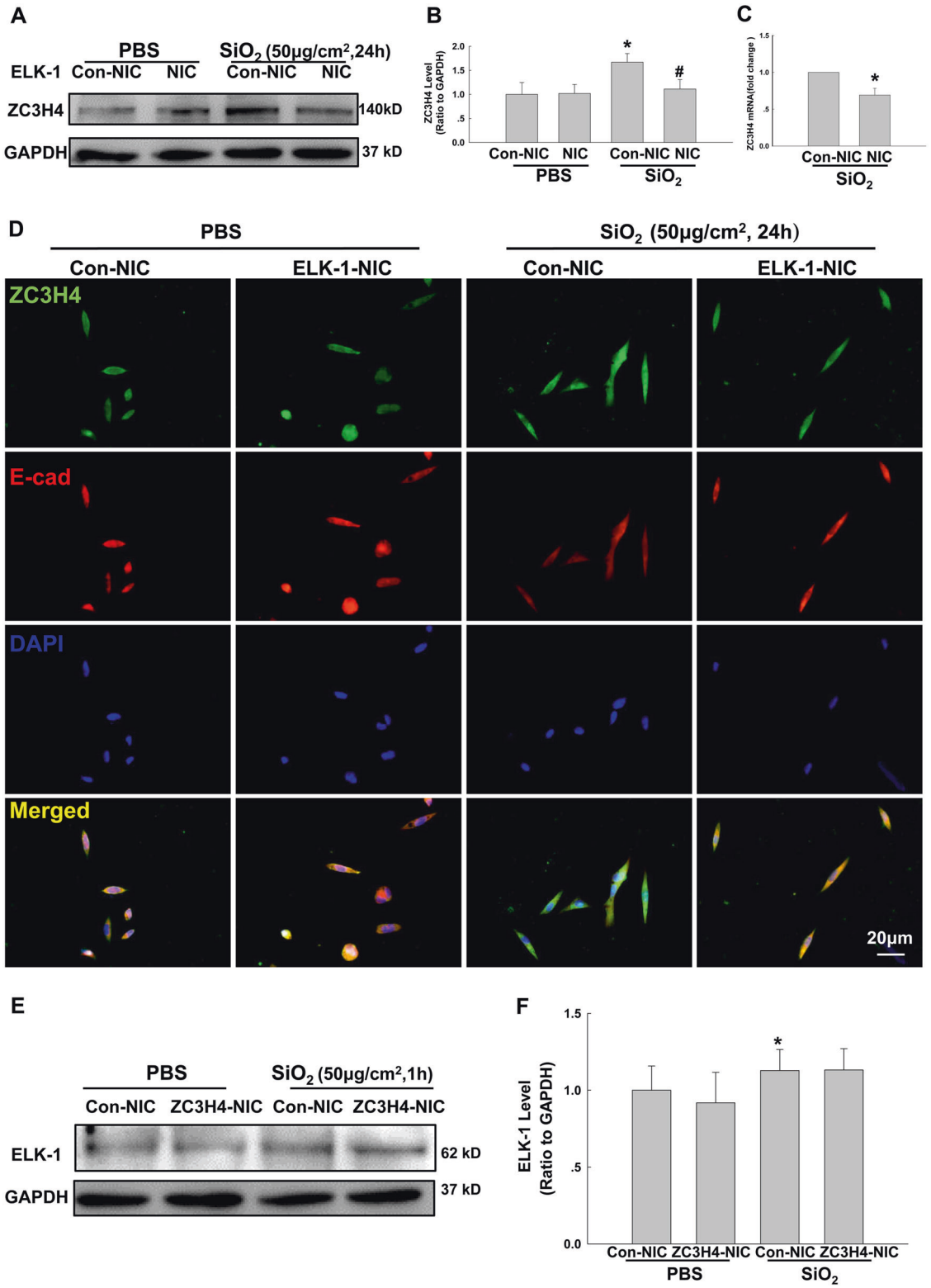

ELK-1/ZC3H4 regulated EMT and TGF-β production

To further confirm the upstream and downstream roles between ELK-1 and ZC3H4 in modulating EMT, ELK-1 ACT plasmids and ZC3H4 NIC plasmids were cotransfected into MLE-12 and BEAS-2B cells. As shown in Figs. 5a, b, S4A, B, EMT and TGF-β production induced by upregulation of ELK-1 expression in MLE-12 and BEAS-2B cells was abolished by treatment with the ZC3H4 NIC plasmid, indicating that ELK-1 regulated EMT and

◀ **Fig. 4 The relevance between ELK-1 and ZC3H4. a** Representative western blots showing that downregulating ELK-1 inhibits SiO_2-induced increase in ZC3H4 expression in MLE-12 cells. **b** Densitometric analyses of ZC3H4 expression in MLE-12 cells ($n = 5$); $^{*}p < 0.05$ vs. the control group; $^{\#}p < 0.05$ vs. the SiO_2 group. **c** Expression of ZC3H4 mRNA, determined by quantitative RT-PCR, is knocked down by ELK-1 NIC in MLE-12 cells; $^{*}p < 0.05$ vs. the ELK-1 control NIC group. **d** Representative immunofluorescence staining images demonstrating that SiO_2 decreases the expression of E-cad and increased the expression of ZC3H4 in MLE-12 cells. CRISPR/Cas9-mediated ELK-1 silencing attenuates the SiO_2-induced increase in ZC3H4 expression and ameliorated the SiO_2-induced decrease in E-cad expression. Scale bar = 20 μm. **e** Representative western blots showing the effect of ZC3H4 NIC on SiO_2-induced ELK-1 expression in MLE-12 cells. **f** Densitometric analyses of five independent experiments showing that ELK-1 expression is upregulated in MLE-12 cells treated with SiO_2 for 1 h under stimulation, and CRISPR/Cas9-mediated ZC3H4 silencing has no effects on ELK-1 expression. $^{*}p < 0.05$ vs. the control group.

TGF-β production via the ZC3H4 protein. These findings were confirmed by immunostaining (Fig. 5c).

ELK-1/ZC3H4 regulated cell functional changes

To investigate the effects of ELK-1/ZC3H4 on modulating functional behaviors related to EMT, we used some functional assays to assess the cotransfection systems. As shown in Fig. 6, overexpression of ELK-1 increased cell viability (Figs. 6a, S4C), proliferation (Figs. 6b, S4D), and migration ability (Fig. 6c, d) in pulmonary epithelial cells, and these effects were significantly reversed by treatment with ZC3H4 NIC plasmids.

Oxidative stress (OS) is involved in EMT via ELK-1 later expression

OS, which represents an imbalanced redox state resulting in increased ROS production and decreased antioxidant ability, has been shown to be an important mediator of persistent inflammatory and fibrotic responses not only associated with the activation of transcriptional factors [43], such as Elk-1, ATF-2, ATF-3, and c-Jun but also with phenotypic changes to epithelial cells [44, 45], such as EMT, cytokines production, proliferation ability, and apoptosis. To evaluate the potential pathogenic mechanisms induced upon silica treatment, the OS index, including ROS levels, and the antioxidant indexes, including SOD and GSH levels, were determined [31]. As shown in Figs. 7a–c, S5A–C, MLE-12 and BEAS-2B cells incubated with SiO_2 for 24 h exhibited higher relative fluorescence intensity, which indicated higher levels of ROS, whereas the SOD and GSH activities were significantly reduced. These results indicated that SiO_2 disturbed the redox balance in epithelial cells. Compelling evidence highlights the crucial role of ROS in EMT and cytokines secretion engagement, so the antioxidant NAC was used to examine the effects of OS on EMT and TGF-β production. The dosage and time of NAC administration were based on the manufacturers' instructions and on previous studies [46, 47]. As shown in Figs. 7d, e, S5D, E, pretreatment with 1 mM NAC markedly inhibited the effect of SiO_2 on EMT and TGF-β production. Moreover, a correlation has been observed between changes in the phosphorylation status of Elk-1 and cellular redox changes [48, 49]. Thus, we further elucidated the potential relevance between the phosphorylation level of Elk-1 and SiO_2-induced OS in epithelial cells. As shown in Figs. 7f, g, S5F, G, compared with the peak time of the Elk-1 phosphorylation at the beginning stage (30–60 min), p-Elk-1 in MLE-12 and BEAS-2B cells were stimulated again to high levels by SiO_2 treatment for 24 h, which seemed to imitate a later period of SiO_2 administration. However, NAC significantly attenuated the SiO_2-induced p-Elk-1. Taken together, these results implied that OS might act as an upstream regulator of the later activation of Elk-1, stimulating EMT and TGF-β production in silicosis.

Discussion

When the lungs are exposed to air containing free silica particles for a long time, the pathologic processes of pulmonary fibrosis begin with impairment and the subsequent limited self-recovery of pulmonary epithelial cells [50, 51], which are closely related to inflammatory cytokine secretion, fibroblast gradual proliferation, and myofibroblast activation. EMT, which is defined by a phenotypic conversion that gives rise to matrix-producing fibroblasts and myofibroblasts, takes part in the generation of new tissue types at the embryonic development stage and plays a vital role in the inflammatory response and wound healing process in damaged tissues. EMT has also been reported to engage in fibrogenesis in tissues such as the kidney [52], heart [53], pulmonary [54], and liver fibrosis [12]. Consistent with our previous findings, the results of this study showed that compared with the control group, the expression level of the typical epithelial marker E-cad was downregulated in epithelial cells of the silica-treated group; at the same time, the expression level of the classical mesenchymal phenotype COL1 was upregulated. These abnormalities in protein expression point to increased EMT in pulmonary fibrosis induced by silica. While, there is a little research that focuses on the pathways or regulators involved in EMT.

The structure of every TCF member is distinguished by three conserved domains: the N-terminal, C-terminal, and B-box regions. The N-terminus is the ETS domain, which

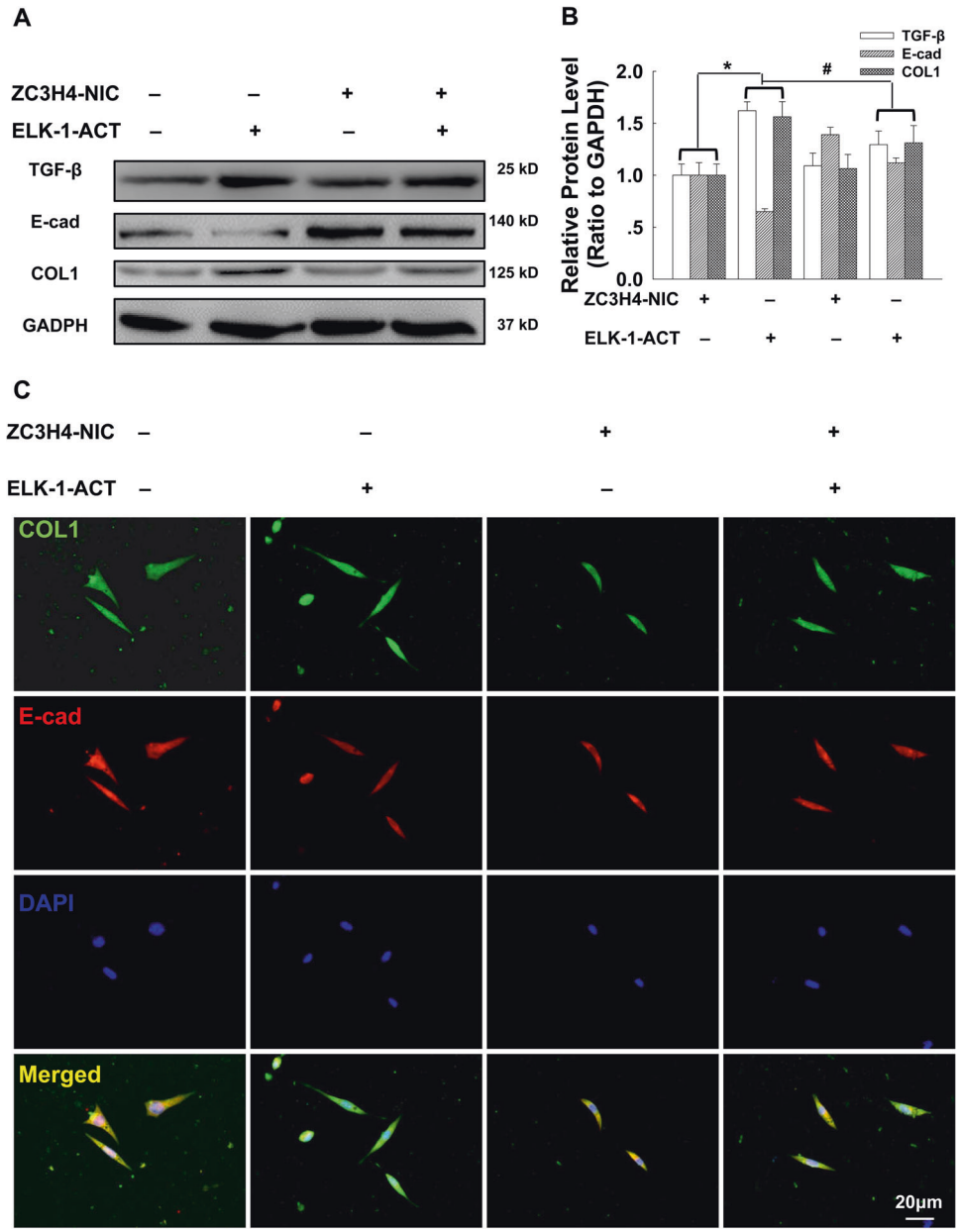

Fig. 5 ELK-1 /ZC3H4 regulates EMT and TGF-β production. a Representative western blots showing the effects of CRISPR/Cas9-mediated ZC3H4 silencing (ZC3H4 NIC) on EMT and TGF-β production induced by ELK-1 ACT in MLE-12 cells. **b** Densitometric analyses of five independent experiments showing that CRISPR/Cas9-mediated ZC3H4 silencing attenuates the ELK-1 ACT-induced increase in Col I expression and TGF-β production, while ameliorates the ELK-1 ACT-induced decrease in E-cad expression; $^{*}p < 0.05$ vs. the control group; $^{\#}p < 0.05$ vs. the ELK-1 ACT group. **c** Representative immunocytochemistry images demostrating that ELK-1 ACT induces the expression of E-cad and increased the expression of Col I. CRISPR/Cas9-mediated ZC3H4 silencing attenuates the ELK-1 ACT-induced EMT in MLE-12 cells. Scale bar = 20 μm.

binds to DNA sequences; the B-box region is postulated to be involved in interaction with SRF; and the C-terminal transcriptional activation domain induces MAPK phosphorylation transduction [55]. ELK-1 is a member of the TCF subfamily of ETS-domain transcription factors that bind to target DNA sites together with an SRF [25]. The DNA-binding activity of many ETS-domain transcription factors is suppressed until appropriate triggers are in place, including phosphorylation and interaction with a coregulatory transcription factor. In addition, Elk-1 has a repression domain that is modified by SUMO to keep it inactivated. It has been postulated that SUMO recruitment of histone deacetylases suppresses the transcriptional activity of Elk-1. Phosphorylation-mediated transduction of signaling pathways, such as the ERK pathway, assists with the de-SUMOylation and p-Elk-1 and stimulates Elk-1 to transition from a transcriptionally suppressive state to an active form. In contrast to the extensive study of the structure of Elk-1, the function of Elk-1 has received little attention by other studies to this point [56]. Our findings were the first to demonstrate that treating pulmonary epithelial cells with SiO_2 dramatically increased the p-Elk-1, as well as its translocation from the cytoplasm to nucleus, suggesting that SiO_2 might mediate a kinase pathway to activate Elk-1. Furthermore, genetic inhibition of Elk-1 with Elk-1 NIC completely abrogated SiO_2-mediated EMT, cell proliferation and migration, suggesting a new function of Elk-1 in epithelial cells and revealing that the activation of

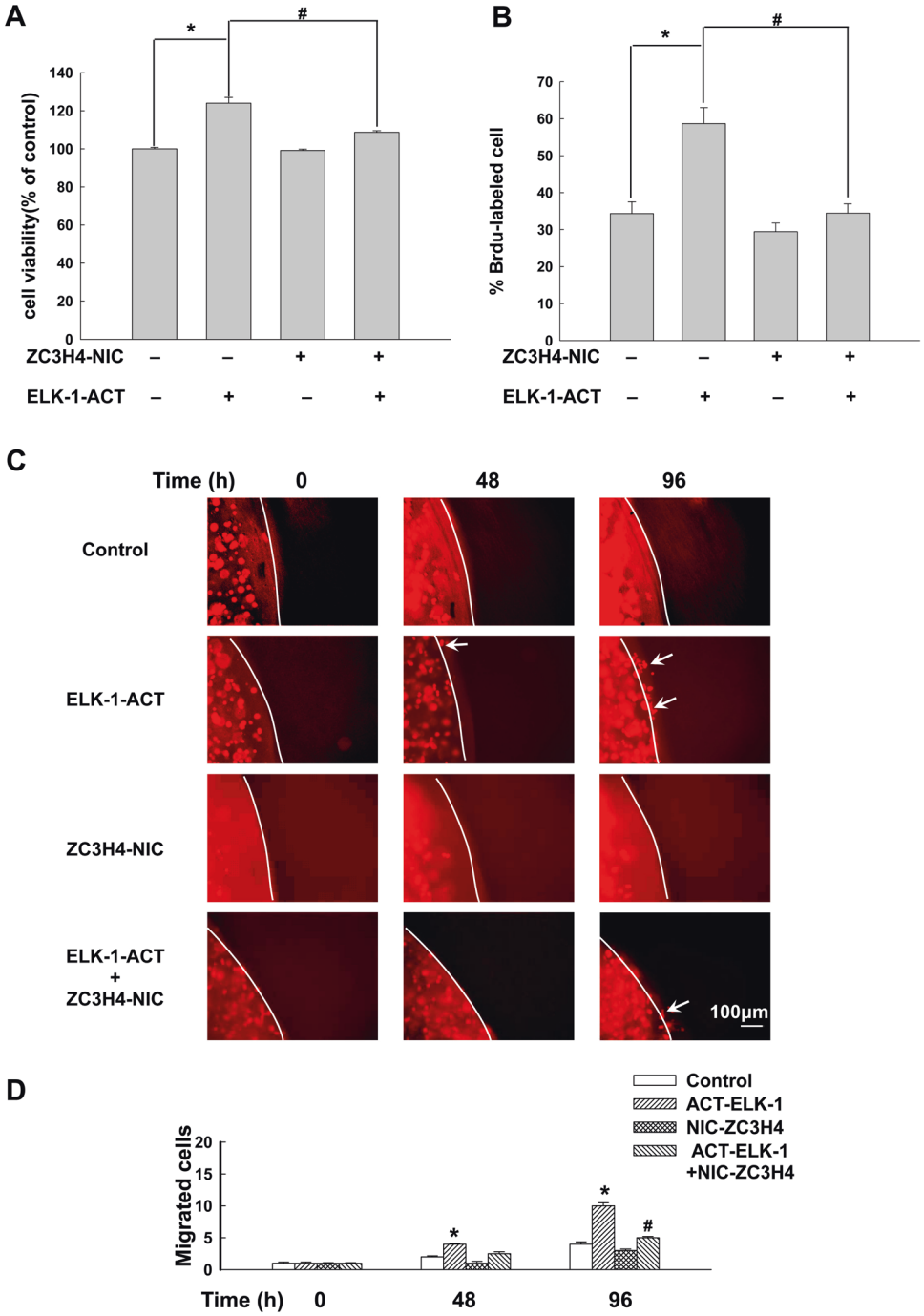

Fig. 6 ELK-1 /ZC3H4 regulates the cell functional changes. a CCK8 assay showing CRISPR/Cas9-mediated ZC3H4 silencing inhibits the increased cell viability induced by ELK-1 ACT in MLE-12 cells. $n = 5$; $^{*}p < 0.05$ vs. the control group; $^{\#}p < 0.05$ vs. the ELK-1 ACT group. **b** Brdu positive-cell counting from five fields per well demonstrating that the increased MLE-12 cells proliferation induced by ELK-1 ACT is attenuated by ZC3H4 silencing; $n = 5$; $^{*}p < 0.05$ vs. the control group; $^{\#}p < 0.05$ vs. the ELK-1 ACT group. **c** Representative images demonstrating the ELK-1 ACT-induced migration of RFP-labeled MLE-12 cells cultured in a 3D matrix, which is abolished by ZC3H4 silencing. Scale bar = 100 μm. **d** Quantification of the number of migrated cells in the 3D migration from six independent experiments. $^{*}p < 0.05$ vs. the control group. $^{\#}p < 0.05$ vs. the ELK-1 ACT group.

Elk-1 might have a significant role in the molecular mechanisms of pulmonary fibrosis.

Accumulating evidence has demonstrated that OS is a potent stimulator of EMT, proliferation, and apoptosis, depending on the cell type and the concentration of oxygen radicals [23]. A previous study reported that reactive oxygen within certain concentrations promote the proliferation and migration of cancer cells [57]. However, another report indicated that OS is involved in EMT and apoptosis of pulmonary epithelial cells [47]. Consistent with the previous study [47], our results indicated that OS stimulated pulmonary EMT induced by SiO_2. Moreover, OS also represents an important factor contributing to the differential activation of transcription factors. As many transcription factors or their interactions are redox-regulated, antioxidant intervention may affect their bioactivity [48]. Elk-1 was regarded as being responsible for SRE induction in response to changes in the cellular redox status induced by treatment with either the oxidant H_2O_2 or various structurally unrelated antioxidants. Our studies provided

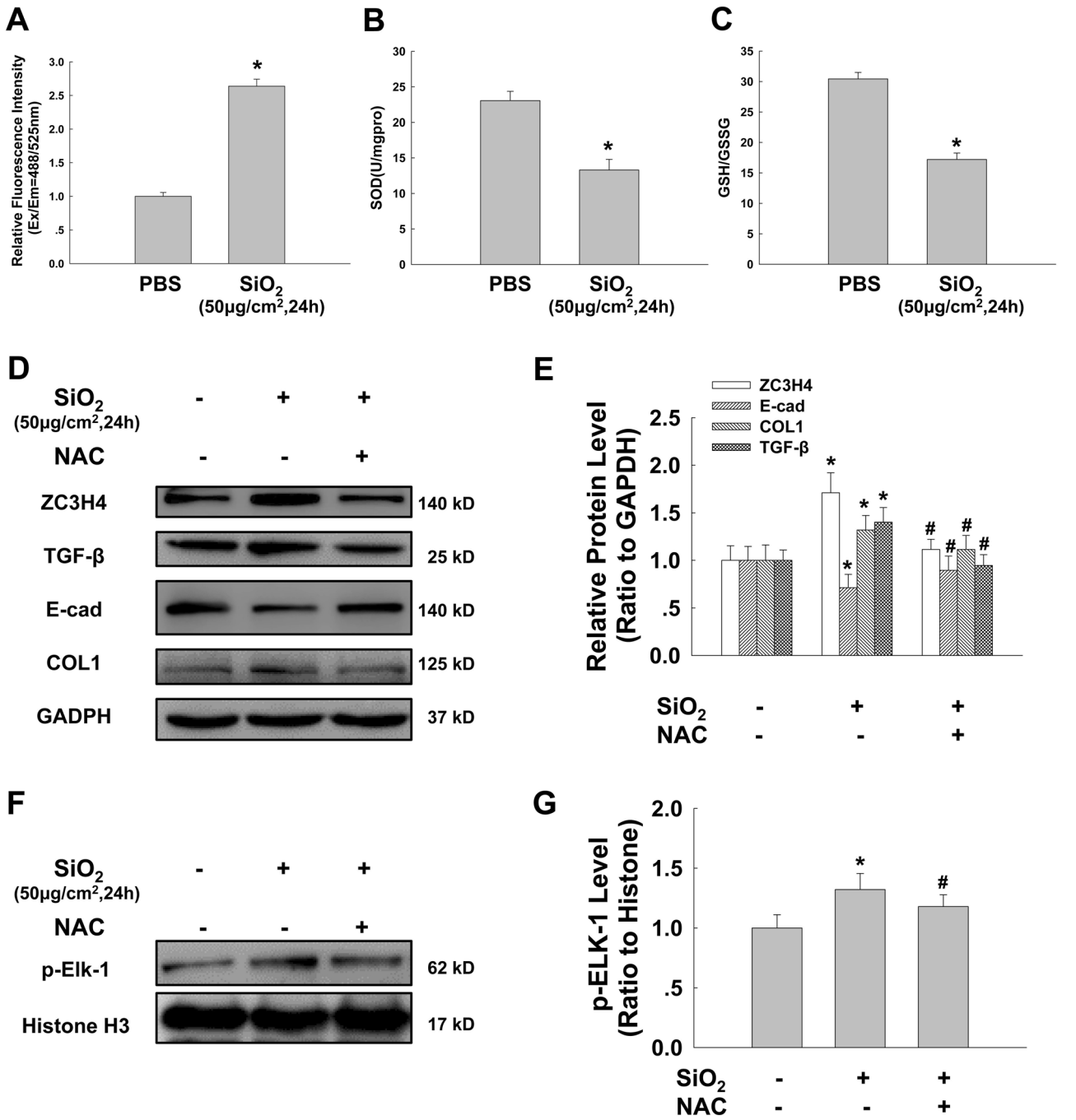

Fig. 7 OS is involved in EMT via ELK-1 later expression. **a** Quantitative results for intracellular ROS levels in MLE-12 cells are determined by relative fluorescence intensity; $n = 5$; $^{*}p < 0.05$ vs. the control group. **b** SiO_2 downregulates SOD activity (U/mg pro) and GSH/GSSG (**c**); $n = 5$; $^{*}p < 0.05$ vs. the control group. MLE-12 cells are pretreated with NAC (1 mM) for 1 h before SiO_2 stimulation for 24 h (**d**–**g**). **d** Representative western blots showing NAC inhibits SiO_2-induced increase in ZC3H4, Col I, and TGF-β expressions, while reverses the SiO_2-induced decrease in E-cad expression. **e** Densitometric analyses of the ZC3H4, Col I, TGF-β, and E-cad expression ($n = 5$); $^{*}p < 0.05$ vs. the control group. $^{\#}p < 0.05$ vs. the SiO_2 group. **f** Representative western blots showing the downregulated phosphorylation of Elk-1 in the nucleus of MLE-12 cells pretreatmented with NAC. **g** Densitometric analyses of Elk-1 phosphorylation ($n = 5$); $^{*}p < 0.05$ vs. the control group. $^{\#}p < 0.05$ vs. the SiO_2 group.

evidence that at the initial stage, the Elk-1 phosphorylation level was upregulated within 3 h of SiO_2 treatment, and then it returned to normal. However, at the later stage after SiO_2 treatment for 24 h, SiO_2 triggered a redox imbalance, which led to the Elk-1 phosphorylation and resulted in an enhanced EMT in epithelial cells.

Elk-1 is also well known as a crucial upstream driver that modulates the transcriptional activation of some specific

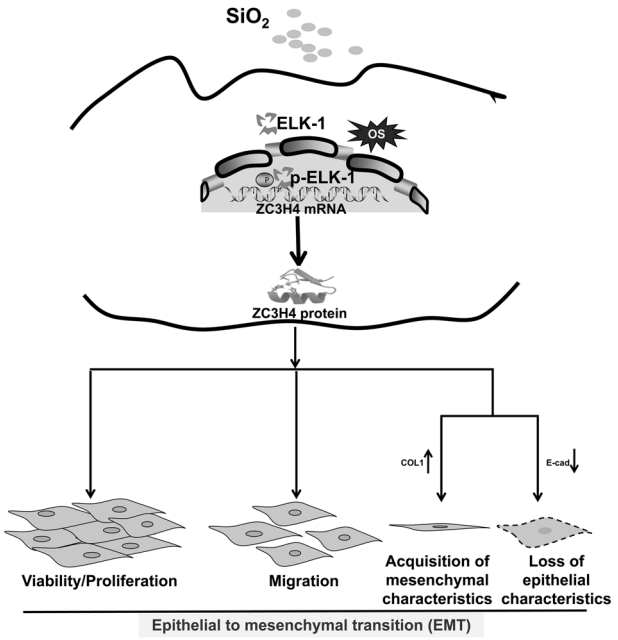

Fig. 8 Schematic diagram showing the detailed molecular mechanisms by which ELK-1 mediates silica-induced EMT. ELK-1 expression is increased in pulmonary epithelial cells exposed to SiO_2, leading to the subsequent downstream activation of ZC3H4 signaling which results in enhanced EMT. Moreover, OS represents an important factor contributing to Elk-1 phosphorylation and resulted in an enhanced EMT in epithelial cells.

downstream genes through phosphorylation-mediated signaling processes [58]. A recent study suggested that Elk-1 can directly activate the expression of the gene *zc3h12a*, which encodes a protein, MCPIP1, that is engaged in the pro-inflammatory response and fibrosis stage. The structure of *zc3h12a* contains an Ets-binding site (binding site for Elk-1) and a CArG box (binding site for the transcription factor SRF), which serve as the basis for the regulation of *zc3h12a* expression by ELK-1 and provide the necessary conditions for triggering expression via the *zc3h12a* promoter [26]. As expected, phosphorylated ELK-1 has been reported to regulate *zc3h12a* gene expression by targeting an SRF binding site in the promoter. ZC3H4 is another member of the CCCH-type zinc finger protein family, and it is critical for the activation and apoptosis of macrophages and for the initiation of EMT after silica exposure [9, 27]. In this study, we measured the expression of ZC3H4 protein and found that it increased significantly after SiO_2 treatment, which was downregulated by Elk-1 inhibition, whereas ZC3H4 NIC did not affect Elk-1 expression; these data suggest that Elk-1 is the upstream regulator of ZC3H4 expression. In addition, knock down of ZC3H4 prevents EMT, and it reduces cell viability, proliferation, and migration induced by Elk-1, implying the interaction between ELK-1 and ZC3H4 regulates EMT and related functional changes in cells. These results demonstrated that *zc3h4* may contain a similar gene structure as MCPIP1, suggesting that ELK-1 can control ZC3H4 expression. Further experiments are needed to confirm the exact regulatory mechanisms between ELK-1 and *zc3h4* gene expression. For example, there may be an SRF binding site or other ELK-1 binding sites on the *zc3h4* gene promoter that mediate the regulatory process, similar to what is found in the *zc3h12a* gene promoter.

To our knowledge, the present study provide the first evidence of the detailed molecular pathways involved in SiO_2-mediated EMT via ELK-1 with upstream activation of OS and downstream activation of ZC3H4 signaling (Fig. 8). These novel findings establish the possibility of using ELK-1 as a potential target in the treatment of silicosis.

Data availability

The obtained results of the current study are available on reasonable request.

Acknowledgements This study is the result of work that was partially supported by the resources and facilities at the core laboratory at the School of Nursing in Nanjing Medical University. RJ designed the experiments, performed the experiments, prepared the figures, wrote the manuscript, and directed the project. QG, MC, and TY performed the experiments and interpreted the data. All authors read, discussed, and approved the final manuscript. We thank all the authors.

Funding Project of "Nursing Science" funded by the Priority Discipline Development Program of Jiangsu Higher Education Institutions (General Office, the People's Government of Jiangsu Province (2018) No.87); Project of "Science and Technology Development" Funded by Nanjing Medical University (NMUB2019023) and Project of "Nursing Science" funded by the Key Discipline Program of Jiangsu Province during the 13th five-year plan (Teaching and Research Office, the People's Government of Jiangsu Province (2016) No. 9).

Author information First and Corresponding author: Rong Jiang, Ph.D., Department of Clinical Nursing, School of Nursing, Nanjing Medical University, Nanjing, Jiangsu, China. E-mail: jiangrong@njmu.edu.cn (or 18205188362@126.com).

Compliance with ethical standards

Conflict of interest The authors declare that they have no conflict of interest.

Ethical approval and consent to participate The Animal Ethics Board of the Nanjing Medical University approved all animal experimental procedures.

References

1. The Lancet Respiratory M. The world is failing on silicosis. Lancet Respir Med. 2019;7:283.

2. Leung CC, Yu IT, Chen W. Silicosis. Lancet. 2012;379:2008–18.
3. Cullinan P, Reid P. Pneumoconiosis. Prim Care Respir J. 2013;22:249–52.
4. Cavalin C, Lescoat A, Ballerie A, Belhomme N, Jego P, Jouneau S, et al. Beyond silicosis, is the world failing on silica hazards? Lancet Respir Med. 2019;7:649–50.
5. Mossman BT, Churg A. Mechanisms in the pathogenesis of asbestosis and silicosis. Am J Respir Crit Care Med. 1998;157:1666–80.
6. Fujimura N. Pathology and pathophysiology of pneumoconiosis. Curr Opin Pulm Med. 2000;6:140–4.
7. Carneiro PJ, Clevelario AL, Padilha GA, Silva JD, Kitoko JZ, Olsen PC, et al. Bosutinib therapy ameliorates lung inflammation and fibrosis in experimental silicosis. Front Physiol. 2017;8:159.
8. Deng H, Xu H, Zhang X, Sun Y, Wang R, Brann D, et al. Protective effect of Ac-SDKP on alveolar epithelial cells through inhibition of EMT via TGF-beta1/ROCK1 pathway in silicosis in rat. Toxicol Appl Pharmacol. 2016;294:1–10.
9. Jiang R, Zhou Z, Liao Y, Yang F, Cheng Y, Huang J, et al. The emerging roles of a novel CCCH-type zinc finger protein, ZC3H4, in silica-induced epithelial to mesenchymal transition. Toxicol Lett. 2019;307:26–40.
10. Yao W, Li Y, Han L, Ji X, Pan H, Liu Y, et al. The CDR1as/miR-7/TGFBR2 axis modulates EMT in silica-induced pulmonary fibrosis. Toxicol Sci. 2018;166:465–78.
11. Fang S, Guo H, Cheng Y, Zhou Z, Zhang W, Han B, et al. circHECTD1 promotes the silica-induced pulmonary endothelial-mesenchymal transition via HECTD1. Cell Death Dis. 2018;9:396.
12. Liu J, Wu Z, Han D, Wei C, Liang Y, Jiang T, et al. MANF inhibits liver cancer via SUMOylation-related suppression of NF-kappaB/Snail signaling pathway and epithelial-mesenchymal transition. Hepatology. 2019. https://doi.org/10.1002/hep.30917.
13. Chang YW, Singh KP. Nicotine-induced oxidative stress contributes to EMT and stemness during neoplastic transformation through epigenetic modifications in human kidney epithelial cells. Toxicol Appl Pharmacol. 2019;374:65–76.
14. Liu Y, Yuan X, Li W, Cao Q, Shu Y. Aspirin-triggered resolvin D1 inhibits TGF-beta1-induced EMT through the inhibition of the mTOR pathway by reducing the expression of PKM2 and is closely linked to oxidative stress. Int J Mol Med. 2016;38:1235–42.
15. Giannoni E, Parri M, Chiarugi P. EMT and oxidative stress: a bidirectional interplay affecting tumor malignancy. Antioxid Redox Signal. 2012;16:1248–63.
16. Dongre A, Weinberg RA. New insights into the mechanisms of epithelial-mesenchymal transition and implications for cancer. Nat Rev Mol Cell Biol. 2019;20:69–84.
17. Barrallo-Gimeno A, Nieto MA. The Snail genes as inducers of cell movement and survival: implications in development and cancer. Development. 2005;132:3151–61.
18. Boutet A, De Frutos CA, Maxwell PH, Mayol MJ, Romero J, Nieto MA. Snail activation disrupts tissue homeostasis and induces fibrosis in the adult kidney. EMBO J. 2006;25:5603–13.
19. Zhao J, Ou B, Han D, Wang P, Zong Y, Zhu C, et al. Tumor-derived CXCL5 promotes human colorectal cancer metastasis through activation of the ERK/Elk-1/Snail and AKT/GSK3beta/beta-catenin pathways. Mol Cancer. 2017;16:70.
20. Hou CH, Lin FL, Hou SM, Liu JF. Cyr61 promotes epithelial-mesenchymal transition and tumor metastasis of osteosarcoma by Raf-1/MEK/ERK/Elk-1/TWIST-1 signaling pathway. Mol Cancer. 2014;13:236.
21. Treisman R. Ternary complex factors: growth factor regulated transcriptional activators. Curr Opin Genet Dev. 1994;4:96–101.
22. Dunn KL, Espino PS, Drobic B, He S, Davie JR. The Ras-MAPK signal transduction pathway, cancer and chromatin remodeling. Biochem Cell Biol. 2005;83:1–14.
23. McCubrey JA, Lahair MM, Franklin RA. Reactive oxygen species-induced activation of the MAP kinase signaling pathways. Antioxid Redox Signal. 2006;8:1775–89.
24. Ye JC, Hsu LS, Tsai JH, Yang HL, Hsiao MW, Hwang JM, et al. MZF-1/Elk-1/PKCalpha is associated with poor prognosis in patients with hepatocellular carcinoma. J Cancer. 2017;8:3028–36.
25. Kasza A. Signal-dependent Elk-1 target genes involved in transcript processing and cell migration. Biochim Biophys Acta. 2013;1829:1026–33.
26. Kasza A, Wyrzykowska P, Horwacik I, Tymoszuk P, Mizgalska D, Palmer K, et al. Transcription factors Elk-1 and SRF are engaged in IL1-dependent regulation of ZC3H12A expression. BMC Mol Biol. 2010;11:14.
27. Yang X, Wang J, Zhou Z, Jiang R, Huang J, Chen L, et al. Silica-induced initiation of circular ZC3H4 RNA/ZC3H4 pathway promotes the pulmonary macrophage activation. FASEB J. 2018;32:3264–77.
28. Zhou Z, Jiang R, Yang X, Guo H, Fang S, Zhang Y, et al. circRNA mediates silica-induced macrophage activation via HECTD1/ZC3H12A-dependent ubiquitination. Theranostics. 2018;8:575–92.
29. Cao Z, Xiao Q, Dai X, Zhou Z, Jiang R, Cheng Y, et al. circHIPK2-mediated sigma-1R promotes endoplasmic reticulum stress in human pulmonary fibroblasts exposed to silica. Cell Death Dis. 2017;8:3212.
30. Islam D, Huang Y, Fanelli V, Delsedime L, Wu S, Khang J, et al. Identification and modulation of microenvironment is crucial for effective mesenchymal stromal cell therapy in acute lung injury. Am J Respir Crit Care Med. 2019;199:1214–24.
31. Cipak Gasparovic A, Milkovic L, Dandachi N, Stanzer S, Pezdirc I, Vrancic J, et al. Chronic oxidative stress promotes molecular changes associated with epithelial mesenchymal transition, NRF2, and breast cancer stem cell phenotype. Antioxidants. 2019;8:E633.
32. Jiang R, Liao Y, Yang F, Cheng Y, Dai X, Chao J. SPIO nanoparticle-labeled bone marrow mesenchymal stem cells inhibit pulmonary EndoMT induced by SiO2. Exp Cell Res. 2019;383:111492.
33. Liu H, Dai X, Cheng Y, Fang S, Zhang Y, Wang X, et al. MCPIP1 mediates silica-induced cell migration in human pulmonary fibroblasts. Am J Physiol Lung Cell Mol Physiol. 2016;310:L121–32.
34. Chen B, Cai HR, Xue S, You WJ, Liu B, Jiang HD. Bile acids induce activation of alveolar epithelial cells and lung fibroblasts through farnesoid X receptor-dependent and independent pathways. Respirology. 2016;21:1075–80.
35. Li L, Xu L, Wen S, Yang Y, Li X, Fan Q. The effect of lncRNA-ARAP1-AS2/ARAP1 on high glucose-induced cytoskeleton rearrangement and epithelial-mesenchymal transition in human renal tubular epithelial cells. J Cell Physiol. 2020. https://doi.org/10.1002/jcp.29512.
36. Marais R, Wynne J, Treisman R. The SRF accessory protein Elk-1 contains a growth factor-regulated transcriptional activation domain. Cell. 1993;73:381–93.
37. Whitmarsh AJ, Shore P, Sharrocks AD, Davis RJ. Integration of MAP kinase signal transduction pathways at the serum response element. Science. 1995;269:403–7.
38. Fazilaty H, Rago L, Kass Youssef K, Ocana OH, Garcia-Asencio F, Arcas A, et al. A gene regulatory network to control EMT programs in development and disease. Nat Commun. 2019;10:5115.

39. Wang L, Tang J, Yang X, Zanvit P, Cui K, Ku WL, et al. TGF-beta induces ST2 and programs ILC2 development. Nat Commun. 2020;11:35.
40. Yang L, Zhang XY, Li K, Li AP, Yang WD, Yang R, et al. Protopanaxadiol inhibits epithelial-mesenchymal transition of hepatocellular carcinoma by targeting STAT3 pathway. Cell Death Dis. 2019;10:630.
41. Wang L, Yu M, Zhao S. lncRNA MEG3 modified epithelial-mesenchymal transition of ovarian cancer cells by sponging miR-219a-5p and regulating EGFR. J Cell Biochem. 2019;120:17709–22.
42. Rencuzogullari O, Yerlikaya PO, Gurkan AC, Arisan ED, Telci D. Palbociclib, a selective CDK4/6 inhibitor, restricts cell survival and epithelial-mesenchymal transition in Panc-1 and MiaPaCa-2 pancreatic cancer cells. J Cell Biochem. 2020;121:508–23.
43. Krifka S, Spagnuolo G, Schmalz G, Schweikl H. A review of adaptive mechanisms in cell responses towards oxidative stress caused by dental resin monomers. Biomaterials. 2013;34:4555–63.
44. Farhat D, Ghayad SE, Icard P, Le Romancer M, Hussein N, Lincet H. Lipoic acid-induced oxidative stress abrogates IGF-1R maturation by inhibiting the CREB/furin axis in breast cancer cell lines. Oncogene. 2020. https://doi.org/10.1038/s41388-020-1211-x.
45. Ko J, Kang HJ, Kim DA, Ryu ES, Yu M, Lee H, et al. Paricalcitol attenuates TGF-beta1-induced phenotype transition of human peritoneal mesothelial cells (HPMCs) via modulation of oxidative stress and NLRP3 inflammasome. FASEB J. 2019;33:3035–50.
46. Zhen J, Yu H, Ji H, Cai L, Leng J, Keller BB. Neonatal murine engineered cardiac tissue toxicology model: Impact of dexrazoxane on doxorubicin induced injury. Life Sci. 2019;239:117070.
47. Yang J, Wang T, Li Y, Yao W, Ji X, Wu Q, et al. Earthworm extract attenuates silica-induced pulmonary fibrosis through Nrf2-dependent mechanisms. Lab Invest. 2016;96:1279–300.
48. Muller JM, Cahill MA, Rupec RA, Baeuerle PA, Nordheim A. Antioxidants as well as oxidants activate c-fos via Ras-dependent activation of extracellular-signal-regulated kinase 2 and Elk-1. Eur J Biochem. 1997;244:45–52.
49. Yan W, Li D, Zhou X. Pravastatin attenuates the action of the ETS domain-containing protein ELK1 to prevent atherosclerosis in apolipoprotein E-knockout mice via modulation of extracellular signal-regulated kinase 1/2 signal pathway. Clin Exp Pharmacol Physiol. 2017;44:344–52.
50. Almale L, Garcia-Alvaro M, Martinez-Palacian A, Garcia-Bravo M, Lazcanoiturburu N, Addante A, et al. c-Met signaling is essential for mouse adult liver progenitor cells expansion after transforming growth factor-beta-induced epithelial-mesenchymal transition and regulates cell phenotypic switch. Stem Cells. 2019;37:1108–18.
51. Chen R, Jin G, Li W, McIntyre TM. Epidermal growth factor (EGF) autocrine activation of human platelets promotes egf receptor-dependent oral squamous cell carcinoma invasion, migration, and epithelial mesenchymal transition. J Immunol. 2018;201:2154–64.
52. Li Y, Hu Q, Li C, Liang K, Xiang Y, Hsiao H, et al. PTEN-induced partial epithelial-mesenchymal transition drives diabetic kidney disease. J Clin Invest. 2019;129:1129–51.
53. Huang T, Barnett JV, Camenisch TD. Cardiac epithelial-mesenchymal transition is blocked by monomethylarsonous acid (III). Toxicol Sci. 2014;142:225–38.
54. Zhou J, Wu P, Sun H, Zhou H, Zhang Y, Xiao Z. Lung tissue extracellular matrix-derived hydrogels protect against radiation-induced lung injury by suppressing epithelial-mesenchymal transition. J Cell Physiol. 2020;235:2377–88.
55. Sharrocks AD. The ETS-domain transcription factor family. Nat Rev Mol Cell Biol. 2001;2:827–37.
56. Yang SH, Sharrocks AD. Convergence of the SUMO and MAPK pathways on the ETS-domain transcription factor Elk-1. Biochem Soc Symp. 2006;73:121–9.
57. Wang J, Lin D, Peng H, Huang Y, Huang J, Gu J. Cancer-derived immunoglobulin G promotes tumor cell growth and proliferation through inducing production of reactive oxygen species. Cell Death Dis. 2013;4:e945.
58. Mylona A, Theillet FX, Foster C, Cheng TM, Miralles F, Bates PA, et al. Opposing effects of Elk-1 multisite phosphorylation shape its response to ERK activation. Science. 2016;354:233–7.